Acta Crystallographica Section D
Biological Crystallography
ISSN 0907-4449

The promiscuous binding of the Fyn SH3 domain to a peptide from the NS5A protein

Jose Manuel Martin-Garcia,[a,b] Irene Luque,[c] Javier Ruiz-Sanz[c] and Ana Camara-Artigas[a]*

[a]Department of Physical Chemistry, Biochemistry and Inorganic Chemistry, University of Almería, Agrifood Campus of International Excellence (ceiA3), Carretera de Sacramento, 04120 Almería, Spain, [b]Department of Chemistry and Biochemistry, Arizona State University, PO Box 871604, Tempe, AZ 85287-1604, USA, and [c]Department of Physical Chemistry and Institute of Biotechnology, Faculty of Sciences, University of Granada, 18071 Granada, Spain

Correspondence e-mail: acamara@ual.es

Received 29 February 2012
Accepted 2 May 2012

PDB References: Fyn-SH3, 3ua6; Fyn-SH3–NS5A, 3ua7.

The hepatitis C virus nonstructural 5A (NS5A) protein is a large zinc-binding phosphoprotein that plays an important role in viral RNA replication and is involved in altering signal transduction pathways in the host cell. This protein interacts with Fyn tyrosine kinase *in vivo* and regulates its kinase activity. The 1.5 Å resolution crystal structure of a complex between the SH3 domain of the Fyn tyrosine kinase and the C-terminal proline-rich motif of the NS5A-derived peptide APPIPPPRRKR has been solved. Crystals were obtained in the presence of $ZnCl_2$ and belonged to the tetragonal space group $P4_12_12$. The asymmetric unit is composed of four SH3 domains and two NS5A peptide molecules; only three of the domain molecules contain a bound peptide, while the fourth molecule seems to correspond to a free form of the domain. Additionally, two of the SH3 domains are bound to the same peptide chain and form a ternary complex. The proline-rich motif present in the NS5A protein seems to be important for RNA replication and virus assembly, and the promiscuous interaction of the Fyn SH3 domain with the NS5A C-terminal proline-rich peptide found in this crystallographic structure may be important in the virus infection cycle.

1. Introduction

Fyn is a member of the Src family of nonreceptor tyrosine kinases and shares the conserved domain structure of this family consisting of consecutive SH3, SH2 and tyrosine kinase (SH1) domains. These enzymes play a critical role in the cell and are tightly regulated (Mayer, 2001): in addition to their regulation through the phosphorylation of key tyrosine residues, the SH3 domain can also mediate regulation of these enzymes through transient interactions with the linker region between the SH2 domain and the kinase domain, in which the canonical P*xx*P binding motif of the SH3 domain is located. In addition, the SH3 domain can also interact with other proteins containing the consensus motif P*xx*P. The observed promiscuous binding of the SH3 domain to different proteins is facilitated by the marked conformational flexibility of the loops around the binding site, the n-Src and RT loops, as well as the distal loop. This conformational flexibility is evident in most of the crystallographic structures of free forms of SH3 domains solved to date, in which the residues present in at least one of these loops show high *B* factors and, in some cases, a lack of electron density in the difference maps (Cámara-Artigas *et al.*, 2010; Martín-García *et al.*, 2007).

Upon binding to the SH3 domain, proline-rich motifs (PRMs) adopt the polyproline type II helical conformation. In this conformation some PRMs show pseudosymmetry, which

Table 1
X-ray data-collection and refinement statistics.

Values in parentheses are for the highest resolution bin.

	Fyn-SH3	Fyn-SH3–NS5A complex
Space group	*C*2	$P4_12_12$
Unit-cell parameters (Å, °)	$a = 72.29$, $b = 47.07$, $c = 42.47$, $\alpha = \gamma = 90$, $\beta = 98.52$	$a = b = 51.32$, $c = 185.6$, $\alpha = \beta = \gamma = 90$
Resolution range (Å)	20–1.85	20–1.50
No. of observations	31205	214698
Unique reflections	11459 (1109)	25757 (3572)
Data completeness (%)	94.1 (62.5)	97.3 (94.0)
$R_{\rm merge}$† (%)	2.7 (15.1)	9.8 (15.7)
$\langle I/\sigma(I)\rangle$	21.7 (3.8)	14.5 (9.8)
Refinement		
No. of protein residues		
Chain *A*	57	63
Chain *B*	59	63
Chain *C*		59
Chain *D*		61
Chain *E*		9
Chain *F*		8
Solvent molecules	86	173
$R_{\rm work}$ (%)	17.5	18.5
$R_{\rm free}$ (%)	24.2	23.1
R.m.s. deviations from ideal geometry		
Bonds (Å)	0.020	0.018
Angles (°)	1.978	1.877
Mean *B* (protein) (Å^2)	19.44	22.99
Ramachandran plot‡: residues in allowed regions (%)	100	100

† $R_{\rm merge} = \sum_{hkl}\sum_i |I_i(hkl) - \langle I(hkl)\rangle|/\sum_{hkl}\sum_i I_i(hkl)$. ‡ From *PROCHECK* (Laskowski *et al.*, 1993).

might allow simultaneous binding to two different SH3 molecules. Additionally, it has been shown that in certain PRMs the charged residues flanking the consensus motif P*xx*P can form salt bridges with those located within the pocket formed by the RT and n-Src loops and that these salt bridges play a relevant role in the orientation of the peptide. Therefore, PRMs with sequences (K/R)*xx*P*xx*P and *x*P*xx*P*x*(K/R) correspond to class I and class II motifs, respectively. The Fyn SH3 domain (Fyn-SH3) is among the SH3 domains which has been described to bind both class I (Morton *et al.*, 1996) and II (Shelton & Harris, 2008) PRMs. The biological implication of this alternative orientation in the binding is still unclear. One commonly raised possibility is that ligand binding in two alternative orientations could open the accessibility of the same PRM to different partners in multi-component protein complexes (Jozic *et al.*, 2005; Moncalián *et al.*, 2006; Hashimoto *et al.*, 2006).

Nonstructural protein NS5A of hepatitis C virus (HCV) is a large zinc-binding phosphoprotein that plays an important role in viral RNA replication and is involved in altering several signal transduction pathways in the host cell (Macdonald *et al.*, 2004). The NS5A protein has been described to be phosphorylated by a still unidentified protein kinase, which is likely to be a proline-directed kinase (He *et al.*, 2006). The protein is constituted of three domains that are connected through flexible linkers. Interestingly, the linker connecting domains II and III contains two motifs with the consensus sequence *x*P*xx*P*x*(K/R). However, these two motifs seem to have evolved differently: the C-terminal motif (PP2.2) is conserved among all HCV genotypes, whereas the N-terminal motif (PP2.1) is not. A detailed analysis of the role played by the proline residues present in both motifs has been performed and the results indicated that some of the prolines are required for RNA replication and also for virus assembly (Hughes *et al.*, 2009).

One of the kinases that is able to bind to the NS5A protein is the Fyn tyrosine kinase (Shelton & Harris, 2008). To better understand the mechanism of the interaction between the C-terminal PRM of the NS5A protein (PP2.2) and the Fyn tyrosine kinase, we have solved the structure of the Fyn SH3 domain complexed with the NS5A peptide APPIPPPRRKR (residues 349–359 of the NS5A sequence). The structure of the Fyn-SH3–NS5A complex has revealed very interesting features which provide new insights into the conformational plasticity of nonreceptor tyrosine kinases and their availability to participate in simultaneous binding to different interaction partners. The promiscuous binding of the NS5A peptide observed in the crystallographic structure of the Fyn-SH3–NS5A complex is of special interest as NS5A is a key protein of HCV and should have relevance to the HCV infection cycle.

2. Materials and methods

2.1. Cloning, expression and purification of the human Fyn SH3 domain

The plasmid pET3d containing the Fyn SH3-domain gene was a generous gift from Dr L. Serrano (CRG, Barcelona). Plasmid-encoded SH3 domain was expressed in *Escherichia coli* BL21 (DE3) strain (Novagen) using 1 m*M* IPTG as the induction agent. Harvested cells were suspended in 100 m*M* Tris buffer pH 9.0 and lysed by two passes through a French pressure cell. The SH3 domain was precipitated from the supernatant with 75% saturated ammonium sulfate and finally resuspended in 50 m*M* sodium phosphate, 500 m*M* sodium chloride buffer pH 6.5. The protein was further purified by size-exclusion chromatography on a Superdex 75 column (GE Healthcare Lifesciences) equilibrated and eluted with the same buffer. SH3 domain-containing fractions were pooled, concentrated and stored at 253 K at above 5 mg ml^{-1} in the same buffer. Protein purity was checked by SDS–PAGE and mass spectrometry and was estimated to be greater than 99%. The Fyn domain is stable for several months under these conditions. The concentration of the Fyn SH3 domain was determined from the absorbance at 280 nm using an extinction coefficient of 16 800 M^{-1} cm^{-1}.

2.2. Peptide ligand

NS5A peptide (APPIPPPRRKR) was purchased from SynBioSci (USA). The peptide was synthesized in the solid phase in an MPS column and was acetylated and amidated at the N- and C-terminus, respectively. The molecular weight was confirmed by mass spectrometry and the peptide purity (>95%) was assessed by analytical HPLC. Peptide stock

solution was prepared in water and its concentration was determined from the absorbance at 220 nm using an extinction coefficient in water of 17 450 M^{-1} cm^{-1} as determined by quantitative amino-acid analysis.

2.3. Isothermal titration calorimetry

Isothermal titration calorimetry (ITC) was performed using a high-precision VP-ITC titration calorimetric system (Microcal Inc., Northampton, Massachusetts, USA). 60 µ*M* Fyn SH3 domain in 20 m*M* sodium phosphate pH 7.0 in the calorimetric cell was titrated with 1.6 m*M* NS5A peptide in the same buffer. A profile of injection volumes ranging from 4 to 20 µl was used. The resulting binding isotherms were analyzed by nonlinear least-squares fitting of the experimental data to a model corresponding to a single set of identical sites, as described by

$$Q = \frac{n[M_t]\Delta HV_0}{2}\left\{1 + \frac{[X_t]}{n[M_t]} + \frac{1}{nK_a[M_t]} - \left[\left(1 + \frac{[X_t]}{n[M_t]} + \frac{1}{nK_a[M_t]}\right)^2 - \frac{4[X_t]}{n[M_t]}\right]^{1/2}\right\}, \quad (1)$$

where Q is the net heat of binding, n is the number of binding sites, K_a is the association constant, V_0 is the active cell volume and $[M]_t$ and $[L]_t$ are the total concentrations of macromolecule and ligand, respectively.

2.4. Dynamic light scattering

Dynamic light-scattering (DLS) measurements were performed at 298 K with a Zetasizer Nano ZS instrument (Malvern Instruments Ltd, United Kingdom) using a 12 µl quartz thermostatted sample cuvette. Protein solutions were prepared at two different concentrations (2 and 12 mg ml^{-1}) in 100 m*M* Tris pH 8.0 in the presence and the absence of $ZnCl_2$. Protein solutions were also prepared at 12 mg ml^{-1} in the presence of the NS5A ligand at a 1:5 molar ratio both in the presence and the absence of $ZnCl_2$. The protein solutions were centrifuged for 40 min at 14 000 rev min^{-1} and sonicated for 1 min immediately before measurement in order to remove any aggregates, dust and possible bubbles from the sample. All samples were analyzed by 25 scans of 35 s duration each. Samples were analyzed after 0, 18 and 27 days of incubation at 298 K. The *DTS* software (Malvern Instruments Ltd) was used to analyse the acquired correlogram (correlation function *versus* time) for calculation of the hydrodynamic radius (R_h).

2.5. Crystallization, data collection, phasing and refinement

Crystals of the Fyn SH3 domain were obtained by optimization of the conditions previously described by Noble *et al.* (1993) and the best crystals grew using the hanging-drop vapour-diffusion method at 298 K by mixing 5 µl protein solution at 15 mg ml^{-1} in 10 m*M* Tris pH 8.0 with 5 µl precipitant solution composed of 5.5 *M* sodium formate, 0.1 *M* MES pH 6. Crystals of the Fyn-SH3–NS5A complex were obtained using the hanging-drop vapour-diffusion method at 298 K by mixing the protein at 15 mg ml^{-1} in 10 m*M* Tris pH 8.0 with the peptide stock solution in a 1:5 molar ratio. Fyn-SH3–NS5A crystals grew using 4 *M* sodium formate, 10 m*M* $ZnCl_2$, 0.1 *M* Tris pH 8.0. For data collection, the crystals were soaked in a cryoprotectant solution containing 10% glycerol, looped and flash-cooled in liquid nitrogen. X-ray diffraction data for the unliganded Fyn SH3 domain were collected with a Bruker Microfocus (Montel Optics) Microstar rotating-anode X-ray generator operated at 45 kV and 60 mA with a kappa CCD detector. X-ray diffraction data for the Fyn-SH3–NS5A complex were collected on beamline ID14-4 of the European Synchrotron Radiation Facility (ESRF) at a wavelength of 0.97 Å using an ADSC Quantum Q315r detector. Data were indexed and integrated using *iMOSFLM* (Battye *et al.*, 2011). Scaling and merging were performed with the *CCP*4 program *SCALA* (Evans, 2006). A summary of the data-collection statistics is shown in Table 1.

The structures were solved using the *CCP*4 software package (Winn *et al.*, 2011). Initial phasing was obtained using the automated molecular-replacement program *MOLREP* (Vagin & Teplyakov, 2010), using the coordinates of the free Fyn SH3 domain (PDB entry 1shf; Noble *et al.*, 1993) without water molecules as a reference model. Cycles of restrained positional refinement with *REFMAC*5 (Murshudov *et al.*, 2011) were alternated with manual building using the resulting σ_A-weighted ($2F_o - F_c$) and ($F_o - F_c$) electron-density maps and the program *Coot* (Emsley & Cowtan, 2004). As several molecules of the Fyn SH3 domain were found in the asymmetric unit, NCS restraints were kept throughout refinement. Water molecules were automatically placed in the difference electron-density maps using the program *Coot*. Besides water molecules, other solvent molecules were identified in the difference electron-density maps. The quality of the structure was checked using the *MolProbity* web server (Chen *et al.*, 2010) and *PROCHECK* (Laskowski *et al.*, 1993). Refinement statistics are collected in Table 1. The coordinates of Fyn-SH3 and Fyn-SH3–NS5A have been deposited in the PDB with accession codes 3ua6 and 3ua7, respectively.

Finally, several programs from the *CCP*4 software package were used to analyze and compare the structures of the unbound Fyn SH3 domain and the Fyn-SH3–NS5A complex: superposition and calculation of r.m.s. deviations of the structures were accomplished using *LSQKAB* and a *B*-factor plot was generated using the program *BAVERAGE* (Winn *et al.*, 2011).

3. Results

3.1. Structure of the human Fyn SH3 domain bound to the NS5A peptide

Crystals of the Fyn-SH3–NS5A complex were obtained using a slight modification of the conditions used to grow the crystals of the free form, although the addition of $ZnCl_2$ seemed to be critical to obtain good-quality diffracting crystals. We found that the Fyn-SH3–NS5A complex crystals belonged to the tetragonal space group $P4_12_12$ and that the

asymmetric unit is formed by four Fyn SH3-domain chains (*A*–*D*) and two NS5A peptide chains (*E* and *F*). Interestingly, each SH3 chain in the asymmetric unit shows a different type of interaction with the NS5A peptide.

Fyn-SH3 *A* and Fyn-SH3 *D* have a molecule of the NS5A peptide bound, but each shows a different peptide orientation. In Fyn-SH3 *A* the orientation of the peptide is N- to C-terminal (Fig. 1*a*), while in Fyn-SH3 *D* the orientation is

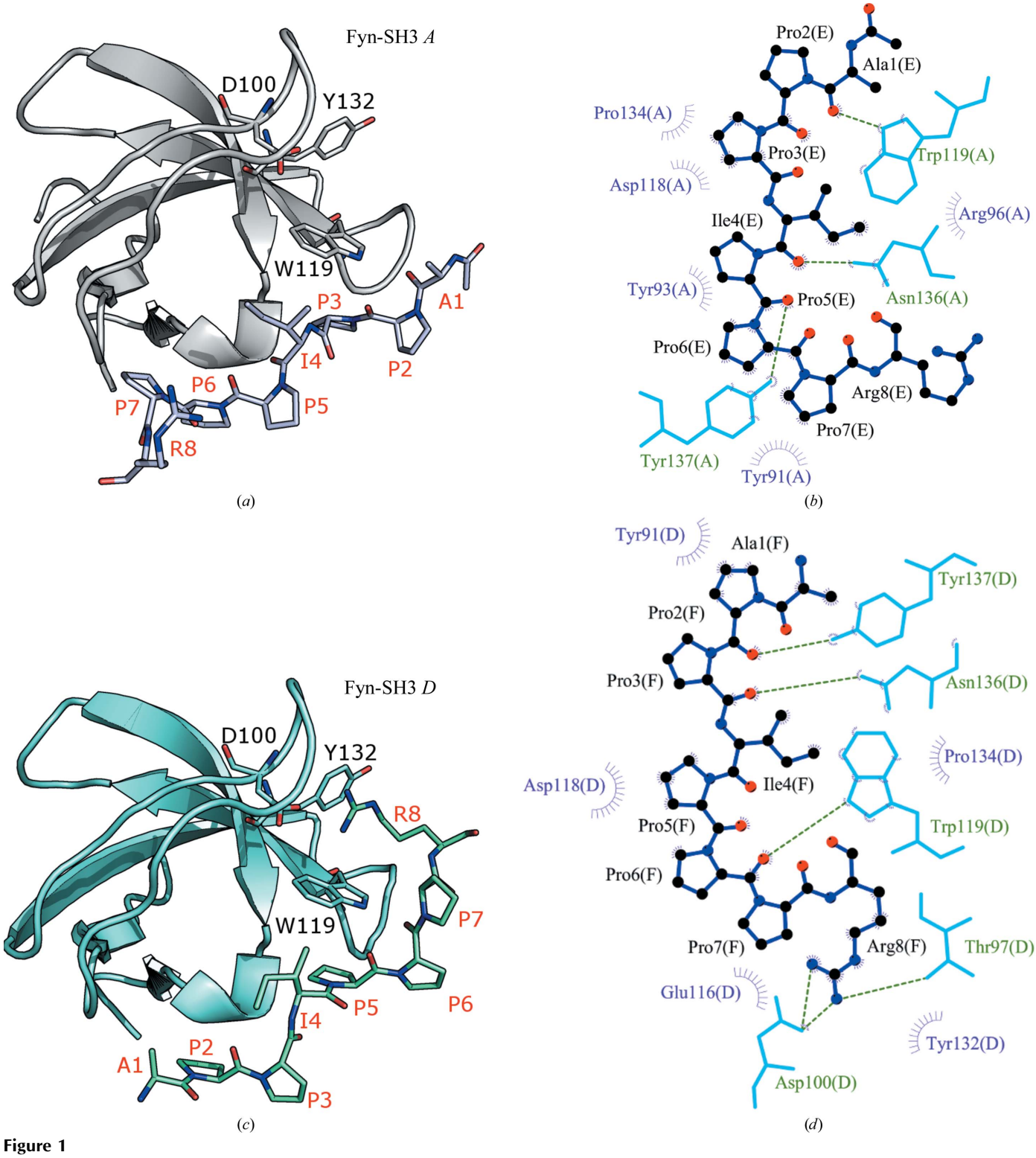

Figure 1
Fyn-SH3 *A* bound to the NS5A peptide (chain *E*) in a class I orientation (*a*) and Fyn-SH3 *D* bound to the NS5A peptide (chain *F*) in a class II orientation (*c*). All figures were produced using *PyMOL* (DeLano, 2002). *LIGPLOT* two-dimensional representations (Wallace *et al.*, 1995) of the interactions between Fyn-SH3 *A* (*b*) and Fyn-SH3 *D* (*d*) with the NS5A peptide are shown.

the opposite: C- to N-terminal (Fig. 1*c*). The NS5A peptide (AP**P**IP**P**P**R**RKR) is a class II peptide and the key arginine residue is placed two residues apart from the canonical P*xx*P motif. We have found that neither of the two NS5A peptide chains present in the asymmetric unit show sufficient electron density for the last three residues in the electron-density maps to be unambiguously modelled. This result is clearly indicative of high flexibility of these residues and therefore they do not establish solid contacts with other residues in the crystal unit cell. This lack of interactions is also in good agreement with previous studies performed with several PRMs also derived from the NS5A protein, where it has been found that Arg356 in the PP2.2 motif (Arg8 in our peptide) plays a critical role in the interaction between the NS5A protein and the Fyn SH3 domain, while the additional positively charged residues present in the C-terminus of the PP2.2 motif do not seem to be crucial for binding (Macdonald *et al.*, 2005).

Within the asymmetric unit, Fyn-SH3 *B* and Fyn-SH3 *C* do not exhibit a bound peptide molecule; however, a detailed inspection of the binding site of Fyn-SH3 *B* shows that peptide chain *E* generated by the symmetry operators is also bound to this SH3 molecule. In this way, peptide chain *E* is bound to Fyn-SH3 *A* and Fyn-SH3 *B* simultaneously (Figs. 2*a* and 2*b*). In addition, the peptide orientation with respect to Fyn-SH3 *B* is C- to N-terminal, the same as the NS5A peptide bound to Fyn-SH3 *D* and as expected from its sequence, which corresponds to a class II peptide. In this way, the pseudo-symmetry observed for the polyproline II helix not only allows the binding of both class I and class II peptides, but also allows concurrent binding to two different Fyn SH3-domain molecules to the same NS5A peptide. Moreover, in either of the two possible orientations, proline and isoleucine side chains fit into the same hydrophobic pockets on the SH3 domain and very similar hydrogen bonds are established from peptide carbonyl groups within the proline-rich ligand.

We found that in peptide chains *E* and *F*, which are bound to Fyn-SH3 *B* and Fyn-SH3 *D*, respectively, residues Ala1–Pro2 and Ile4–Pro5 interact with the binding pockets outlined by residues Tyr91–Tyr137 (first pocket) and Trp119–Pro134–Asn136 (second pocket), respectively (Figs. 1*c* and 1*d*). In addition, Arg8 and Asp100 establish a salt bridge in the third pocket. All these interactions are characteristic of class II peptides. Interestingly, in the Fyn-SH3–NS5A complexes with a class II orientation, in addition to the salt bridge described previously, the positively charged guanidinium group of the arginine residue adopts a parallel orientation with respect to the plane of the aromatic side chain of Tyr132 (Fig. 1*c*). This interaction can be described as a cation–π interaction, a strong noncovalent binding interaction, and its contribution to protein–ligand interactions has been reported (Wu & McMahon, 2008).

The interactions between Fyn-SH3 *A* and the *E* peptide molecule (class I peptide orientation) results in the packing of residues Pro6–Pro7 in the first pocket and residues Ile4–Pro3 in the second pocket. No interactions were found between the arginine residues present in the peptide and the SH3-domain residues belonging to Fyn-SH3 *A* (Figs. 1*a* and 1*b*). Therefore, when comparing each Fyn-SH3–NS5A complex present in the unit cell, the main difference observed is the salt bridge established between Arg8 of the peptide and Asp100 located in the RT loop of the SH3 domain, which favours the class II peptide orientation found in Fyn-SH3 *B* and Fyn-SH3 *D*. In our crystallographic structure the major differences between the three different Fyn-SH3–NS5A complexes found in the asymmetric unit are located in the conformation of the residues of the peptide that are implied in binding. The r.m.s.d. value obtained on superimposition of the peptide molecules is 1.2 Å and the major difference is located at residue Ile4 (r.m.s.d. value of 2.6 Å). In this way Ile4 can accommodate its side chain to fit better to both SH3 domains simultaneously

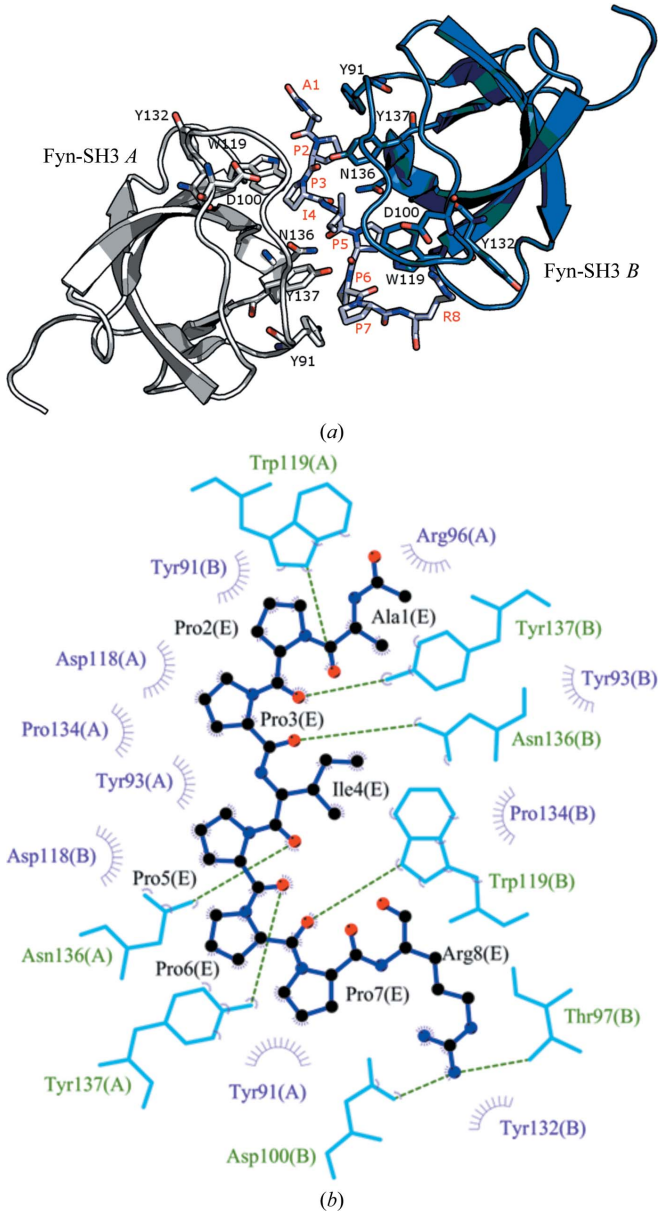

(*a*)

(*b*)

Figure 2
(*a*) Heterotrimeric complex formed by Fyn-SH3 chain *A* (white) and chain *B* (blue) bound to peptide chain *E* (grey). (*b*) *LIGPLOT* two-dimensional representation (Wallace *et al.*, 1995) of the interactions between Fyn-SH3 chains *A* and *B* and NS5A chain *E* in the heterotrimeric complex.

and allow optimization of the hydrogen bonds formed at the binding interface (Fig. 2).

3.2. Structure of the human Fyn SH3 domain

The structure of the Fyn SH3 domain is a good example of the high flexibility exhibited by the loops in most of the unbound crystallographic structures of SH3 domains solved to date (Cámara-Artigas, Martín-García *et al.*, 2009; Cámara-Artigas *et al.*, 2011; Martín-García *et al.*, 2007; Palencia *et al.*, 2010). The asymmetric unit of the Fyn-SH3 domain is composed of two molecules, *A* and *B*, and the most significant difference between them appears in the n-Src loop. When we compared our structure with that previously reported by Noble and coworkers (PDB entry 1shf; Noble *et al.*, 1993), the r.m.s.d. between the *A* chains was 0.6 Å and that between the *B* chains was 0.9 Å; these values are clearly lower than the r.m.s.d. value obtained when the *A* and *B* chains of the same structure are compared (1.6 Å). In both structures the n-Src loop residues 112–118 are modelled in a different conformation in each of the two molecules present in the asymmetric unit. These differences could be ascribed to a lack of electron density in the difference maps to model the backbone of the n-Src loop residues in chain *B*, while in chain *A* the backbone of the loop is well defined. However, it is worth noting that the lack of electron density preventing modelling of the *B*-chain backbone would only explicitly affect three residues: Ser114, Ser115 and Glu116. Nevertheless, comparison of our structure with the previously reported structure deposited with PDB code 1shf (Noble *et al.*, 1993) shows appreciable differences in the positions modelled for some residues whose positions are well defined in our electron-density maps. These residues are located in the n-Src and the RT loops, which play a key role in the affinity and the specificity of the interaction between these SH3 domains and the PRMs, and their flexibility might contribute to a better fitting of the peptide into the binding site (Wittekind *et al.*, 1994; Arold *et al.*, 1998).

In addition, some noticeable changes in the side-chain conformations of aromatic residues located in the binding site have been found between chains *A* and *B*. These differences can be attributed to the orientation of the side chains to favour the packing as well as crystal contacts; they also show the high plasticity of the binding site of the Fyn SH3 domain. For example, differences in the position of the Trp119 side chain allow a cation–π interaction of the aromatic ring of this residue in chain *B* with the guanidinium group of Arg123 in chain *A* of a symmetry-related molecule. At the same time, this residue also forms a salt bridge with Asp100 in chain *B*. These crystalline contacts, which mimic the Asp100–Arg8 interaction in the Fyn-SH3–NS5A complex, are not present in the side chain of Trp119 belonging to chain *A*. As noted above, cation–π interactions seem to play a relevant role in the binding of the NS5A peptide and also other arginine-containing peptides. For example, in the crystal structure of the complex formed by Fyn-SH3 and the VSL12 peptide the arginine residue bound to Asp100 also interacts with Trp119 (Fyn-SH3–VSL12 complex structure, PDB entry 4eik; A. Cámara-Artigas, unpublished work). Consequently, these interactions would also play an important role in crystal packing.

3.3. Comparison of the structures of the unbound Fyn SH3 domain and of the Fyn SH3 domain bound to the NS5A peptide

Comparison of the two chains present in the unbound Fyn SH3-domain structure and those present in the Fyn-SH3–NS5A complex shows that the main difference between the chains is found in the n-Src loop conformation. We have found that the n-Src loop conformation in the *A* chain of the unbound domain is more similar to those present in the *A*, *B* and *D* chains of the complex structure. Additionally, as expected, the most noticeable changes are located at residues Tyr91, Tyr137 and Trp119, which are directly involved in the binding of the proline residues of the canonical binding motif P*xx*P. Therefore, we can infer that these conformational changes of the side chains at the binding site may be important for binding of the peptide. Following this rationale, the ability of some SH3 domains to bind peptides in different orientations has been attributed to a specific conserved tryptophan, which would be assigned as Trp119 in the Fyn-SH3 sequence (Fernandez-Ballester *et al.*, 2004). Interestingly, on comparing the Trp119 position in the *A* and *B* chains of the unbound structure, we found a significant displacement of the side chain of this residue in each chain, with an r.m.s. deviation significantly larger than 1 Å for the side-chain atoms of this residue. Nevertheless, superimpositions of all of the chains present in the complex structure and the *A* chain of the unbound structure showed only a slight displacement of this tryptophan (less than 0.5 Å). Equivalent displacements have been found for tyrosine residues present in the first pocket of the binding site (Tyr91 and Tyr137).

Fyn-SH3 *C* in the Fyn-SH3–NS5A complex structure, which appears to be unbound, shows a similar displacement of the aromatic residues present in the binding site, but the most prominent feature of Fyn-SH3 *C* is that some residues located in the n-Src loop also seem to be disordered. These differences cannot be attributed to changes in the contribution of the residues belonging to the n-Src loop to crystal contacts. All of the Fyn SH3 domains in the Fyn-SH3–NS5A complex structure show some residues of this loop participating in crystal contacts. Moreover, in the unbound structure these residues also participate in crystal contacts in both chains. Our results reveal that the n-Src loop shows a high flexibility in the unbound form and that upon binding to PRMs this loop adopts a more restricted conformation. Additionally, these findings seem to indicate that chain *A* of the unbound structure is more similar to the bound Fyn SH3-domain chains found in the Fyn-SH3–NS5A complex.

3.4. Dynamic light-scattering experiments reveal that the Fyn SH3 domain is a dimer in solution in the presence of zinc ions

To test the aggregation state in solution of unbound Fyn SH3 domain and of that complexed with the NS5A peptide,

we carried out a set of DLS experiments at several protein concentrations ranging from 2 to 12 mg ml^{-1} both in the presence and the absence of Zn^{2+} ions. In the absence of Zn^{2+} the only macromolecular species present in the solution showed a hydrodynamic radius of 1.5–1.7 nm at all protein concentrations assayed, which indicated no dimerization in solution for either the unbound Fyn SH3 domain or the Fyn-SH3–NS5A complex. This same behaviour has previously been reported for the c-Src SH3 domain (Camara-Artigas, Martín-García *et al.*, 2009) and for the α-Spc SH3 domain even at very high protein concentrations (Camara-Artigas, Andújar-Sánchez *et al.*, 2009). In contrast, upon the addition of 10 m*M* $ZnCl_2$ to solutions of the unbound Fyn SH3 domain and the Fyn-SH3–NS5A complex the hydrodynamic radius of both proteins increased to 2.9 nm, indicating that the only populated macromolecular species in solution was a dimer (Fig. 3).

The interaction between SH3 domains giving rise to dimeric structures has previously been reported (Maignan *et al.*, 1995; Delbrück *et al.*, 2002; Nishida *et al.*, 2001; Kristensen *et al.*, 2006). In spite of the structural information currently available for the Fyn SH3 domain in unbound and bound states (Noble *et al.*, 1993; Musacchio *et al.*, 1994; Morton *et al.*, 1996; Renzoni *et al.*, 1996; Demers & Mittermaier, 2009; Lee *et al.*, 1996; Arold *et al.*, 1997, 1998; Franken *et al.*, 1997), this is the first time that homodimerization in the presence of zinc ions in solution has been described for this specific SH3 domain. However, such an arrangement has previously been observed in other SH3 domains both *in vitro* and *in vivo* (Kishan *et al.*, 1997; Delbrück *et al.*, 2002; Guijarro *et al.*, 1998; Nishida *et al.*, 2001; Harkiolaki *et al.*, 2003; Romir *et al.*, 2007). For example, in the crystal structures of Mona/Gads (Harkiolaki *et al.*, 2003) and Lck (Romir *et al.*, 2007) the observed dimerization has been attributed to binding of Zn^{2+} to these proteins.

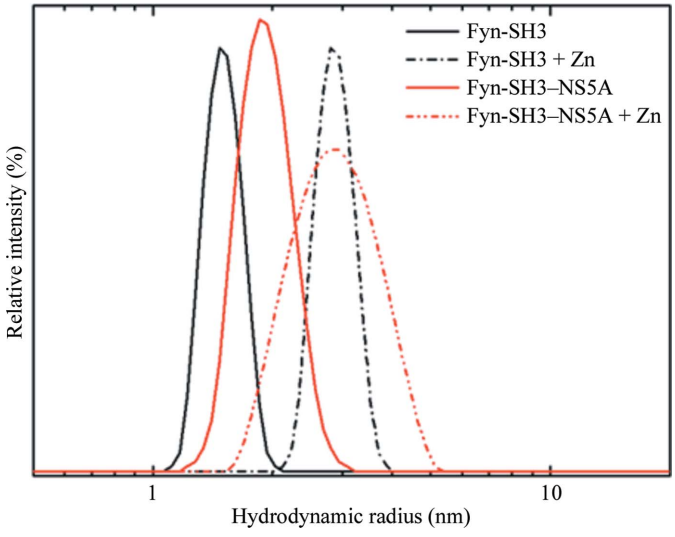

Figure 3
DLS measurements of the hydrodynamic radius distribution of the species present in solution for the Fyn SH3 domain (12 mg ml^{-1}) and its complex with the NS5A peptide in the absence (solid lines) and the presence (dashed lines) of Zn^{2+}.

3.5. Interfacial zinc in the crystal contacts of the Fyn-SH3–NS5A complex

The presence of two large peaks (>8σ) in the electron-density maps near a contact between SH3-domain chains indicates the occurrence of a metal-binding site. As $ZnCl_2$ was present in the precipitant solution used to obtain the Fyn-SH3–NS5A crystals, two zinc ions were modelled at these sites. Both zinc sites show the typical tetrahedral coordination in which the ions are linked through the side chains of residues His104 and Glu107 from one monomer and the His104 side chain from a symmetry-related molecule. One of the sites is present in Fyn-SH3 *C*, where the symmetry-related His104 belongs to Fyn-SH3 *A*. The other zinc site is located in Fyn-SH3 *D* and in this case the symmetry-related His104 belongs to Fyn-SH3 *B*. We have also modelled a formate ion from the precipitant solution as the fourth ligand in both zinc sites (see Fig. 4). In this way, the asymmetric unit seems to be composed of two dimers of the Fyn SH3 domain linked through zinc ions.

The positions of these zinc ions within the crystal contact might explain why the crystal structure of Fyn-SH3–NS5A was solved using crystals grown in the presence of $ZnCl_2$. In fact, the presence of a stable dimer in the solution precedes the nucleation and further growth of these crystals, as inferred from the results of the DLS experiments, and this behaviour has previously been reported for other SH3 domains (Cámara-Artigas, Andújar-Sánchez *et al.*, 2009; Cámara-Artigas, Martín-García *et al.*, 2009; Cámara-Artigas *et al.*, 2011).

3.6. Isothermal titration calorimetry: binding energetics of NS5A to the Fyn SH3 domain

The energetics of the interaction between the Fyn SH3 domain and the NS5A peptide were measured by calorimetric techniques. Fig. 5 shows the results of calorimetric titration at 298 K in 20 m*M* sodium phosphate pH 7.0. The thermodynamic analysis reveals that the binding of NS5A to the Fyn

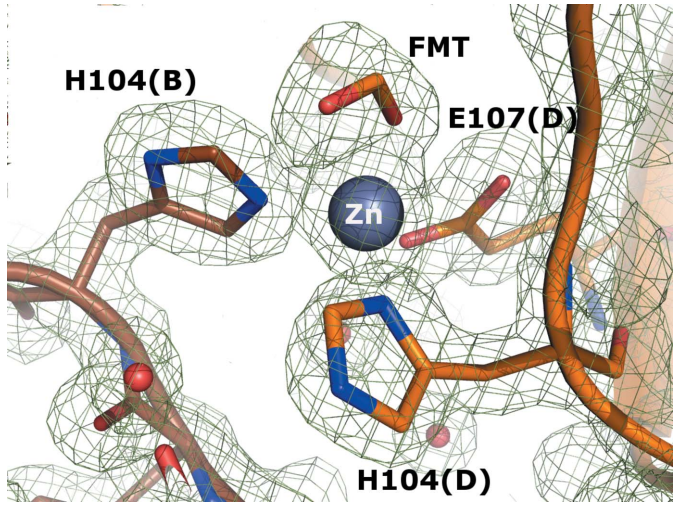

Figure 4
$2F_o - F_c$ electron-density difference map contoured at 1σ for the Zn-binding site. The zinc site is formed by Glu107 and His104 from chain *D* and His104 from chain *B*. The fourth ligand is a formate ion.

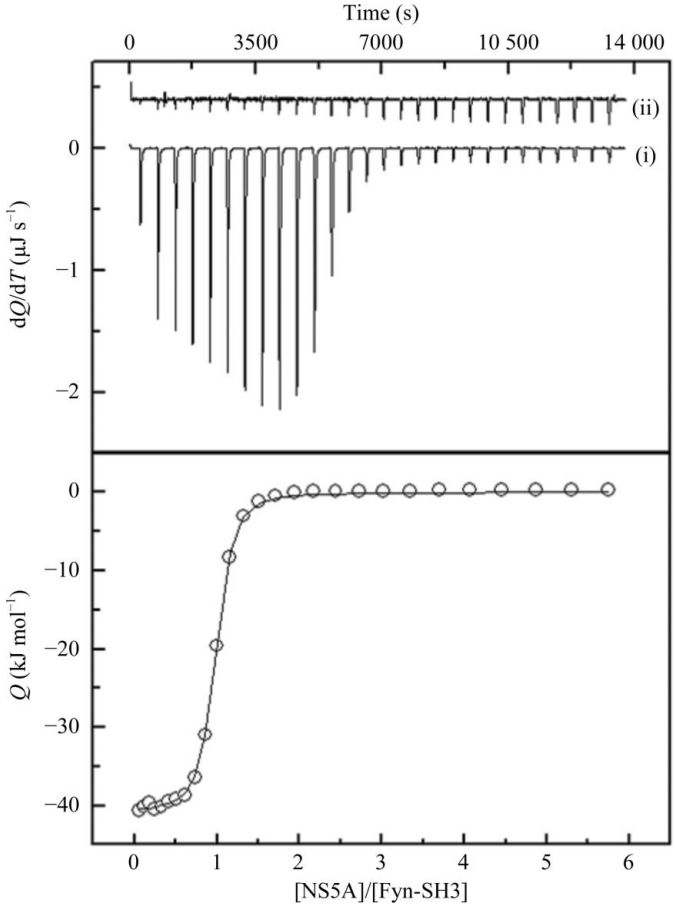

Figure 5
Calorimetric titration of the Fyn SH3 domain with the proline-rich ligand NS5A in 20 m*M* sodium phosphate pH 7.0. Upper panel: (i) heat effects associated with the injection of the ligand into a calorimetric cell containing the Fyn SH3 domain at 60 μ*M*, (ii) dilution experiments of the ligand into the corresponding buffer under the same conditions and with an identical injection profile. Lower panel: ligand-concentration dependence of the heat released upon binding after normalization and correction for the heats of dilution. Symbols represent experimental data and the solid line correspond to the best fitting to a model considering one set of binding sites (equation 1).

SH3 domain is driven by a favourable enthalpy change ($\Delta H = -41.0$ kJ mol^{-1}), which is partially compensated by an unfavourable entropic contribution ($-T\Delta S = 5.0$ kJ mol^{-1}). The stoichiometry of binding is 1:1.

Titration of the Fyn SH3 domain with the NS5A peptide yielded a dissociation constant of 0.62 μ*M*, which is in full agreement with that previously reported for the full-length NS5A protein by surface plasmon resonance (SPR) experiments (Shelton & Harris, 2008). This result suggests that the determinants of the binding affinity of the full NS5A protein for the Fyn SH3 domain are completely coded into the sequence of the NS5A ligand (APPIPPPRRKR). Additionally, the stoichiometry of binding indicates that in solution only one mole of peptide is bound per mole of SH3 domain.

4. Discussion

A quite unusual and very interesting feature of the crystallographic structure of the Fyn-SH3–NS5A complex is that the asymmetric unit is composed of four SH3 chains, with each one representing a different interaction with the peptide. The singularity of this crystallographic structure allows us to study not only the conformational changes between the bound and unbound SH3 domain, but also the conformational changes associated with binding of the same peptide in two opposite orientations.

Another remarkable feature found in the Fyn-SH3–NS5A structure is that peptide chain *E* is shared by Fyn-SH3 *A* and Fyn-SH3 *B*. The symmetry of the NS5A PPII helix, together with the recognition of PRMs in two alternate orientations, lets the SH3 domain recognize a binding motif on the surface of another SH3 domain. It is important to point out that this is the first time that the recognition of the same peptide molecule by two Fyn SH3-domain molecules has been reported. Nevertheless, a close inspection of the structure of the Fyn-SH3–3BP-2 complex (PDB code 1fyn) shows that a representation of the symmetry-related counterparts results in the superposition of the 3BP-2 peptide chain modelled with the symmetry-generated chain (Musacchio *et al.*, 1994); to account for the modelling of the peptide molecule at a special position, the whole peptide was refined using 0.5 occupancy.

The simultaneous interaction of two SH3 domains with a single peptide molecule has also been described in the crystal structures of the SH3 domains of CIN85 and β-PIX in complex with a proline-arginine peptide from Cbl-b (Jozic *et al.*, 2005), the N-terminal SH3 domain of CMS in complex with Cbl-b (Moncalián *et al.*, 2006) and the cortactin SH3 domain in complex with the P4 peptide from AMAP1 (Hashimoto *et al.*, 2006). In these heterotrimeric complexes, one SH3 domain is bound to the peptide in a class I orientation, whereas the second SH3 domain is bound in a class II orientation, and the critical roles of the arginine/lysine residues in the formation of these complexes have been verified using point mutants (Moncalián *et al.*, 2006). For example, in the β-PIX–Cbl-b complex there are two critical arginine residues in the Cbl-b peptide, Arg904 and Arg911, which form two salt bridges with the Asp23 and Glu24 residues, respectively, in the RT loop of the SH3 domain. In addition, this crystal structure also shows that these arginine residues are located between two tryptophan residues, Trp43 and Trp54. The same type of interactions can be found in the CIN85–Cbl-b crystal structure, in which Asp16 and Glu17 also establish salt bridges with Arg904 and Arg911; in this complex the side chain of Trp36 is located at a distance of 4–5 Å from the guanidinium group.

The crystallographic structure of the Fyn-SH3–NS5A complex allows us to model the position of the arginine residue of the NS5A peptide, the interaction of which is critical for the peptide orientation (Arg8). Our data show that in addition to the salt bridge between Arg8 and Asp100, the cation–π interaction with Trp119 must also be taken into account. This interaction could be modified by the residue present at position 132, and its importance in driving the orientation of the peptide in class I or II has previously been reported (Fernandez-Ballester *et al.*, 2004). In our case, both residues (Trp119 and Tyr132) play a relevant role in the interaction since these two residues establish cation–π inter-

actions with the arginine residue of the peptide and this hypothesis is supported by our ITC results (results not shown). The thermodynamic signature of the titration of the Fyn SH3 domain with the NS5A peptide is similar to those found for similar calorimetric titrations of SH3 domains, with negative values for both the binding enthalpy and entropy (Palencia *et al.*, 2004, 2010). However, non-water molecules have been found in the interface of the binding site of the Fyn-SH3–NS5A complex which can account for the negative contribution to the enthalpy value. The cation–π interactions established between the arginine residue and aromatic residues in the binding site might account to some extent for the negative enthalpic contribution to the binding energetics. To support this, experimental ΔG° values for cation–π interactions have been measured using model systems and theoretical calculations have predicted that the contribution of cation–π interactions to protein–peptide recognition can be as strong as those of salt bridges and hydrogen bonds (Pletneva *et al.*, 2001). In the absence of buried water molecules, this interaction would account for the negative value observed for the enthalpy change associated with binding of the NS5A peptide to the Fyn SH3 domain. Previous studies conducted with the Fyn SH3-domain Y132A mutant have shown that Tyr132 has a significant impact on the binding of Fyn-SH3 to NS5A (Shelton & Harris, 2008).

Cation–π interactions can also be found in other Fyn-SH3–peptide complex structures. For example, in the Fyn-SH3–Nef protein complex, which is another class II complex, the arginine residue present in the Nef protein forms a salt bridge to Asp100 and a hydrogen bond to Tyr132. Moreover, it also shows the guanidinium group packed against the planar Trp119 ring (Arold *et al.*, 1997; Lee *et al.*, 1996). In the case of the class I complex structure of the Fyn SH3 domain bound to P2L solved by NMR techniques (Renzoni *et al.*, 1996), the average NMR structure of the Fyn-SH3–P2L complex (PDB entry 1azg) does not show any interaction of the key arginine residue (Arg93) of the P2L peptide with the SH3 domain. However, a close inspection of each model within the ensemble of modelled structures (PDB entry 1a0n; Renzoni *et al.*, 1996) clearly shows a large discrepancy between the different positions modelled for this arginine residue. In some of the modelled conformations the side chain of the arginine residue is in close contact with the Asp100 and Trp119 side chains, but in some other conformations it also interacts with Tyr132.

Some clues to the promiscuous nature of the interaction between the NS5A peptide and the Fyn SH3 domain can be obtained if we take into account the mechanism proposed by Demers & Mittermaier (2009). This mechanism, which was proposed for the binding of PRMs flanked by positive residues, consists of two stages: the first step involves the rapid formation of an electrostatic interaction of an acidic residue in the RT loop with a positively charged residue flanking the consensus motif P*xx*P and the second step involves the docking of the peptide into the shallow pockets formed by the aromatic residues in the binding site. In the Fyn-SH3–NS5A complex the first step would be the formation of the electrostatic interaction between Asp100 and the corresponding arginine residue in the peptide: Arg8 in the NS5A peptide. The second step of the mechanism proposed by Demers and Mittermaier, the close contact between the peptide residues with those in the binding site, might favour the formation of hydrogen-bond interactions that may also contribute partially to the favourable enthalpy change and the unfavourable entropy change observed in the ITC experiments. The negative entropy value obtained could be attributed to conformational changes in both the peptide and the SH3 domain which are needed for better fitting of the peptide into the hydrophobic binding pocket. This loss of backbone entropy upon binding in the SH3 domain is supported by dynamics studies performed on binding of the RLP2 peptide to the c-Src SH3 domain by means of NMR (Wang *et al.*, 2001).

The presence of a ternary complex in the unit cell of the crystal structure of the Fyn-SH3–NS5A complex raised the question of the actual presence of this complex in solution. In ITC characterization of the heterotrimeric complex of CIN85 and the proline-arginine peptide from Cbl-b, the binding isotherms showed a binding stoichiometry of 1:0.57. Additionally, in this ternary complex an arginine residue has been proposed to play a relevant role in peptide-induced dimerization as well as in the binding affinity (Jozic *et al.*, 2005). Nevertheless, calorimetric titration of the Fyn SH3 domain with the NS5A peptide showed a 1:1 stoichiometry and this result is also in agreement with the presence of a monomer of the Fyn SH3 domain and its complex with NS5A in solution as shown by DLS experiments. However, the presence of a ternary complex in our crystallographic structure points to the possibility of simultaneous binding of two different SH3 domains to the same polyproline II helix. Thus, in our case, the presence of the ternary complex between Fyn-SH3 *A*, Fyn-SH3 *B* and NS5A chain *E* seems to be favoured by the experimental conditions used to crystallize the Fyn-SH3–NS5A complex, in which high concentrations of the protein were used. Nonetheless, its presence in our crystal structure reveals that under suitable conditions this ternary complex would be thermodynamically favoured and opens the possibility of the additional binding of another SH3 molecule to an already bound peptide. The entropic cost of formation of the PPII helix would not be present in the binding of the second SH3 molecule and the high concentration of the SH3 domain present in the crystallization solution may favour binding (Cámara-Artigas, Martín-García *et al.*, 2009).

In addition to the peculiar arrangement of the Fyn-SH3 and NS5A peptide molecules found in the asymmetric unit of the crystallographic structure, it is worth noting that crystals of the complex were only obtained in the presence of Zn^{2+} ions. The role of zinc ions in modulation of the binding of Fyn tyrosine kinase to the NS5A protein has not yet been studied; however, a Zn^{2+}-binding site has been described in the NS5A protein (Tellinghuisen *et al.*, 2005). The Zn^{2+} ion coordinated to His104 and Glu106 is situated at the end of the RT loop at a distance of approximately 20 Å from the binding site. However, it has been reported that the entire SH3 domain actively participates in modulation of the binding of PRMs

(Wang *et al.*, 2001). The binding of this Zn^{2+} ion can play a role in tuning the switching on and off of the interactions of these domains with different partners in the cell and the propagation of the ligand-binding process beyond the SH3–ligand interface.

Finally, we want to point towards the possible consequences of the promiscuous interactions of the Fyn SH3 domain with the NS5A peptide. The NS5A protein interacts not only with other viral proteins, but also with host-cell proteins. This viral protein has been described to interfere in cellular pathways and processes, including innate immunity and host-cell growth and proliferation. The Fyn tyrosine kinase is one of the enzymes of the host cell that participates in signal cascades. In most tyrosine kinases the intramolecular interactions of the SH3 with the PRM present in the SH2-kinase linker is weak, and other proteins with PRM-containing sequences, such as for example the NS5A protein, can favourably compete for SH3-domain binding. As a consequence of this intermolecular binding, the tyrosine kinase retains its activity by disrupting the intramolecular constraints. The high affinity constant value measured for binding of the NS5A peptide to the Fyn SH3 domain supports the finding that the interaction of the NS5A protein with the Fyn tyrosine kinase leads to its activation (Macdonald *et al.*, 2004). Additionally, the crystal structure of the Fyn-SH3–NS5A complex shows that only slight changes in the NS5A peptide conformation allow its simultaneous binding to two different SH3 domains to form a ternary complex. It is worth noting that the formation of this ternary complex is favoured by the conditions used to obtain the crystals and has not been detected in solution under the conditions used in this work. However, the presence of this ternary complex in the crystal structure indicates that under specific conditions it is thermodynamically stable and may also be present in the cell. This association might play some role in the formation of multiprotein complexes, as has previously been reported for other SH3 domains (Jozic *et al.*, 2005; Moncalián *et al.*, 2006; Hashimoto *et al.*, 2006). Along these lines, the participation of the Src tyrosine kinase in multiprotein complexes of the HCV has recently been reported and this association has been proposed to play a relevant role in virus replication (Pfannkuche *et al.*, 2011). However, there is some controversy about the real role of several members of the Src tyrosine kinase family in HCV replication (Pfannkuche *et al.*, 2011; Macdonald *et al.*, 2004, 2005; Shelton & Harris, 2008; Hughes *et al.*, 2009). The highly conserved nature of the PP2.2 motif present in the NS5A protein suggests an important role of this PRM, most likely in altering the cellular environment of the host cell to favour virus persistence. A better knowledge of the interactions established between the PRMs present in the HCV proteins and SH3 domains at the molecular level will provide a better understanding of their role in virus replication and how the viral proteins can affect the signal cascade of the host cell.

This work was performed by members of the BIO-328 and FQM-171 research groups of the Andalusian Regional Government (Spain). We would also like to thank the Factoría Española de Cristalización (Ingenio/Consolider 2010 grant) for the use of its X-ray diffraction facility. We would also like to thank Dr Andrés Palencia for assistance in measurement of the crystals on beamline ID14-4 (ESRF, Grenoble, France). This research was funded by the Spanish Ministry of Education and Sciences and FEDER (EU) (BIO2009-13261-C02-01/02) and the Andalusian Regional Government (Spain) and FEDER (EU) (P09-CVI-5063 and P10-CVI-5915). We would also like to thank beamline ID14-4 at the European Synchrotron Radiation Facility (ESRF), Grenoble, France for funding (MX-1225).

References

Arold, S., Franken, P., Strub, M.-P., Hoh, F., Benichou, S., Benarous, R. & Dumas, C. (1997). *Structure*, **5**, 1361–1372.
Arold, S., O'Brien, R., Franken, P., Strub, M.-P., Hoh, F., Dumas, C. & Ladbury, J. E. (1998). *Biochemistry*, **37**, 14683–14691.
Battye, T. G. G., Kontogiannis, L., Johnson, O., Powell, H. R. & Leslie, A. G. W. (2011). *Acta Cryst.* D**67**, 271–281.
Cámara-Artigas, A., Andújar-Sánchez, M., Ortiz-Salmerón, E., Cuadri, C. & Casares, S. (2009). *Acta Cryst.* D**65**, 1247–1252.
Cámara-Artigas, A., Andújar-Sánchez, M., Ortiz-Salmerón, E., Cuadri, C., Cobos, E. S. & Martin-Garcia, J. M. (2010). *Acta Cryst.* F**66**, 1023–1027.
Cámara-Artigas, A., Gavira, J. A., Casares, S., Garcia-Ruiz, J. M., Conejero-Lara, F., Allen, J. P. & Martinez, J. C. (2011). *Acta Cryst.* D**67**, 189–196.
Cámara-Artigas, A., Martín-García, J. M., Morel, B., Ruiz-Sanz, J. & Luque, I. (2009). *FEBS Lett.* **583**, 749–753.
Chen, V. B., Arendall, W. B., Headd, J. J., Keedy, D. A., Immormino, R. M., Kapral, G. J., Murray, L. W., Richardson, J. S. & Richardson, D. C. (2010). *Acta Cryst.* D**66**, 12–21.
DeLano, W. L. (2002). *PyMOL*. http://www.pymol.org.
Delbrück, H., Ziegelin, G., Lanka, E. & Heinemann, U. (2002). *J. Biol. Chem.* **277**, 4191–4198.
Demers, J. P. & Mittermaier, A. (2009). *J. Am. Chem. Soc.* **131**, 4355–4367.
Emsley, P. & Cowtan, K. (2004). *Acta Cryst.* D**60**, 2126–2132.
Evans, P. (2006). *Acta Cryst.* D**62**, 72–82.
Fernandez-Ballester, G., Blanes-Mira, C. & Serrano, L. (2004). *J. Mol. Biol.* **335**, 619–629.
Franken, P., Arold, S., Padilla, A., Bodeus, M., Hoh, F., Strub, M.-P., Boyer, M., Jullien, M., Benarous, R. & Dumas, C. (1997). *Protein Sci.* **6**, 2681–2683.
Guijarro, J. I., Morton, C. J., Plaxco, K. W., Campbell, I. D. & Dobson, C. M. (1998). *J. Mol. Biol.* **276**, 657–667.
Harkiolaki, M., Lewitzky, M., Gilbert, R. J., Jones, E. Y., Bourette, R. P., Mouchiroud, G., Sondermann, H., Moarefi, I. & Feller, S. M. (2003). *EMBO J.* **22**, 2571–2582.
Hashimoto, S. *et al.* (2006). *Proc. Natl Acad. Sci. USA*, **103**, 7036–7041.
He, Y., Staschke, K. A. & Tan, S.-L. (2006). *Hepatitis C Viruses: Genomes and Molecular Biology*, edited by S.-L. Tan, pp. 267–292. Norwich: Horizon Bioscience.
Hughes, M., Gretton, S., Shelton, H., Brown, D. D., McCormick, C. J., Angus, A. G., Patel, A. H., Griffin, S. & Harris, M. (2009). *J. Virol.* **83**, 10788–10796.
Jozic, D., Cárdenes, N., Deribe, Y. L., Moncalián, G., Hoeller, D., Groemping, Y., Dikic, I., Rittinger, K. & Bravo, J. (2005). *Nature Struct. Mol. Biol.* **12**, 972–979.
Kishan, K. V. R., Scita, G., Wong, W. T., Di Fiore, P. P. & Newcomer, M. E. (1997). *Nature Struct. Biol.* **4**, 739–743.
Kristensen, O., Guenat, S., Dar, I., Allaman-Pillet, N., Abderrahmani, A., Ferdaoussi, M., Roduit, R., Maurer, F., Beckmann, J. S.,

Kastrup, J. S., Gajhede, M. & Bonny, C. (2006). *EMBO J.* **25**, 785–797.
Laskowski, R. A., MacArthur, M. W., Moss, D. S. & Thornton, J. M. (1993). *J. Appl. Cryst.* **26**, 283–291.
Lee, C.-H., Saksela, K., Mirza, U. A., Chait, B. T. & Kuriyan, J. (1996). *Cell*, **85**, 931–942.
Macdonald, A., Crowder, K., Street, A., McCormick, C. & Harris, M. (2004). *J. Gen. Virol.* **85**, 721–729.
Macdonald, A., Mazaleyrat, S., McCormick, C., Street, A., Burgoyne, N. J., Jackson, R. M., Cazeaux, V., Shelton, H., Saksela, K. & Harris, M. (2005). *J. Gen. Virol.* **86**, 1035–1044.
Maignan, S., Guilloteau, J.-P., Fromage, N., Arnoux, B., Becquart, J. & Ducruix, A. (1995). *Science*, **268**, 291–293.
Martín-García, J. M., Luque, I., Mateo, P. L., Ruiz-Sanz, J. & Cámara-Artigas, A. (2007). *FEBS Lett.* **581**, 1701–1706.
Mayer, B. J. (2001). *J. Cell Sci.* **114**, 1253–1263.
Moncalián, G., Cárdenes, N., Deribe, Y. L., Spínola-Amilibia, M., Dikic, I. & Bravo, J. (2006). *J. Biol. Chem.* **281**, 38845–38853.
Morton, C. J., Pugh, D. J., Brown, E. L., Kahmann, J. D., Renzoni, D. A. & Campbell, I. D. (1996). *Structure*, **4**, 705–714.
Murshudov, G. N., Skubák, P., Lebedev, A. A., Pannu, N. S., Steiner, R. A., Nicholls, R. A., Winn, M. D., Long, F. & Vagin, A. A. (2011). *Acta Cryst.* D**67**, 355–367.
Musacchio, A., Saraste, M. & Wilmanns, M. (1994). *Nature Struct. Biol.* **1**, 546–551.
Nishida, M., Nagata, K., Hachimori, Y., Horiuchi, M., Ogura, K., Mandiyan, V., Schlessinger, J. & Inagaki, F. (2001). *EMBO J.* **20**, 2995–3007.
Noble, M. E., Musacchio, A., Saraste, M., Courtneidge, S. A. & Wierenga, R. K. (1993). *EMBO J.* **12**, 2617–2624.
Palencia, A., Cámara-Artigas, A., Pisabarro, M. T., Martínez, J. C. & Luque, I. (2010). *J. Biol. Chem.* **285**, 2823–2833.
Palencia, A., Cobos, E. S., Mateo, P. L., Martínez, J. C. & Luque, I. (2004). *J. Mol. Biol.* **336**, 527–537.
Pfannkuche, A., Büther, K., Karthe, J., Poenisch, M., Bartenschlager, R., Trilling, M., Hengel, H., Willbold, D., Häussinger, D. & Bode, J. G. (2011). *Hepatology*, **53**, 1127–1136.
Pletneva, E. V., Laederach, A. T., Fulton, D. B. & Kostic, N. M. (2001). *J. Am. Chem. Soc.* **123**, 6232–6245.
Renzoni, D. A., Pugh, D. J., Siligardi, G., Das, P., Morton, C. J., Rossi, C., Waterfield, M. D., Campbell, I. D. & Ladbury, J. E. (1996). *Biochemistry*, **35**, 15646–15653.
Romir, J., Lilie, H., Egerer-Sieber, C., Bauer, F., Sticht, H. & Muller, Y. A. (2007). *J. Mol. Biol.* **365**, 1417–1428.
Shelton, H. & Harris, M. (2008). *Virol. J.* **5**, 24.
Tellinghuisen, T. L., Marcotrigiano, J. & Rice, C. M. (2005). *Nature (London)*, **435**, 374–379.
Vagin, A. & Teplyakov, A. (2010). *Acta Cryst.* D**66**, 22–25.
Wallace, A. C., Laskowski, R. A. & Thornton, J. M. (1995). *Protein Eng.* **8**, 127–134.
Wang, C., Pawley, N. H. & Nicholson, L. K. (2001). *J. Mol. Biol.* **313**, 873–887.
Winn, M. D. *et al.* (2011). *Acta Cryst.* D**67**, 235–242.
Wittekind, M., Mapelli, C., Farmer, B. T., Suen, K. L., Goldfarb, V., Tsao, J., Lavoie, T., Barbacid, M., Meyers, C. A. & Mueller, L. (1994). *Biochemistry*, **33**, 13531–13539.
Wu, R. & McMahon, T. B. (2008). *J. Am. Chem. Soc.* **130**, 12554–12555.